Acc. Chem. Res. **1998,** *31,* 567−573

Inducing and Viewing Bond Selected Chemistry with Tunneling Electrons

WILSON HO

Laboratory of Atomic and Solid State Physics and Materials Science Center, Cornell University, Ithaca, New York 14853

Received August 13, 1997

Introduction

Chemical and biological reactions can be described as a series of reaction steps, each involving the dissociation or the formation of a single bond. The effects of the environment, e.g., neighboring bonds and molecules, the solvent, or the substrate, are considered as perturbations to the bonds, affecting their structure, energy, and dynamics. While these effects can be extremely important, the ability to describe the changes occurring in each individual bond provides an indication of how well we understand the reactions. Furthermore, reactions involving large molecules are often predominantly confined to specific bonds in a localized area of the molecule, the active site.

To date, the study of the chemistry of individual bonds has been carried out in two important ways: supersonic molecular beams[1] and femtosecond lasers (femtochemistry).[2] In the first, the reaction between two molecular species occurs in the collision region between molecular beams, and the products are probed as a function of the incident and scattering angles, energies, and alignment of the molecules. In the latter, the reaction of a molecule in a molecular beam is initiated by a femtosecond laser pulse and its progress is probed by a second femtosecond laser pulse. Molecular collisions are infrequent in a molecular beam, allowing the study of chemical reactions involving isolated molecules. The dynamics and the reaction time scales of individual bonds can then be probed rigorously.

In 1959, R. P. Feynman challenged us to pursue "a new field of physics" by stating that "The problems of chemistry and biology can be greatly helped if our ability to see what we are doing, and to do things on an atomic level, is ultimately developed—a development which I think cannot be avoided."[3] The invention of the scanning tunneling microscope[4] (STM) has allowed us to meet this challenge, as was first demonstrated in atomic and molecular manipulations.[5,6] The STM and related scanning probes, most notably the atomic force microscope[7] (AFM), have allowed us to probe the structure of materials and chemical reactions with atomic resolution. Since its conception, the range of applications of STM and AFM have far exceeded their original intentions.[8]

The STM provides spatially resolved images of the uppermost layer of a solid; the images reflect the coupling between the electronic states of the STM tip and the surface at a particular energy selected by the applied voltage bias between the tip and the surface. Dramatic images of the atomic arrangements have been obtained for both metal and semiconductor surfaces. In some cases, especially for small adsorbed molecules, it is possible to map out the molecular orbitals near the Fermi level. The imaging capabilities of the STM are derived from the exponential dependence of the tunneling current on the tip−surface separation and the proximity of the tip to the surface (about 5−7 Å).

In addition to imaging, the STM can be used to induce chemistry. The combination of imaging and chemistry is one of the most exciting applications of the STM. Control of chemistry with spatial resolution less than 1 Å can be achieved in the initiation of the reaction and imaging of the reactants and products. The STM is used to induce and view bond-selected chemistry at the limit of the spatial resolution (subangstrom), and "angstrochemistry" has been suggested as a concise description of this new area of study.[9] Although angstrochemistry involves the study of molecules adsorbed on solid surfaces, many of the concepts and understanding are expected to be transferable to chemistry in the gas phase and in solutions.

It should be pointed out that the requirement of an atomically resolved probe is a necessary but insufficient condition for carrying out angstrochemistry. For example, atomic imaging has been achieved with the scanning transmission electron microscope[10,11] (STEM) and the field ion microscope[12] (FIM) many years prior to the invention of STM. Although electrons in the state-of-the-art STEM can be confined to dimensions of a few angstroms, their extremely high energies (order of 100 keV) cause surface deteriorations and indiscriminate excitations of the molecules in the beam.[13,14] In FIM, the sample is confined to be a sharp tip and experiments are restricted to those of atomic desorption under high electric fields; single-bond selectivity and activation within an adsorbed molecule is difficult. To achieve angstrochemistry, the instrument needs to be capable of imaging with atomic resolution *and* be able to selectively confine the initial excitation to a specific chemical bond. For it to be practical and versatile, manipulation is also desirable. The STM is such an instrument. Tunneling electrons form an

Wilson Ho was born in Taiwan in 1953. He received his B.S. and M.S. degrees in chemistry from the California Institute of Technology in 1975 and his Ph.D. degree in physics from the University of Pennsylvania in 1979. After a brief period at the Bell Laboratories, he was attracted in 1980 to the natural beauty of Ithaca and is currently Professor of Physics. His research group is probing molecules adsorbed on solid surfaces with scanning tunneling microscopes and femtosecond lasers and is growing semiconductor thin films for materials research and device fabrication.

S0001-4842(95)00178-6 CCC: $15.00
Published on Web 05/15/1998

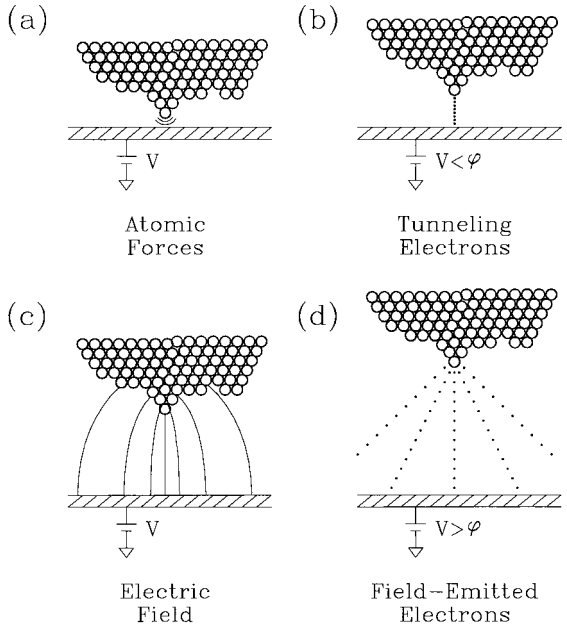

FIGURE 1. Schematic showing the basic manipulation mechanisms in STM. The separation between the tip and the sample is a scaled representation. *V* is the applied bias voltage and φ is the work function of the sample.

effective excitation source for inducing chemistry. It is in effect an ultrasmall electron beam welder for making and breaking single bonds.

Mechanisms of Chemistry Induced by STM

The STM consists of a sharp metal tip held in close proximity to a conducting substrate by feedback electronics.[15] The fact that single atoms can be resolved on metal and semiconductor surfaces suggests that the tunneling electrons are confined to atomic dimensions. The single most important property of the STM is the exponential dependence of the magnitude of the tunneling current on the tip−sample distance (z) for a fixed voltage difference (bias) between the tip and the sample.[16] Since STM images do not always directly reflect the positions of the atomic nuclei, the interpretation of the images often requires theoretical modeling.[17−19]

The exponential dependence of the tunneling current on the separation between the surface and tip atoms makes it possible to position the tip precisely at a chosen distance above the surface. The different mechanisms of single atom/molecule manipulation and chemistry can then be explored by proper combinations of two of the three experimental variables (the third is determined by the other two): tip−sample distance, bias voltage, and current.

There are four basic mechanisms underlying the spatially resolved manipulation and chemistry with the STM as depicted in Figure 1, which involve the atomic forces, tunneling electrons, electric field, and field-emitted electrons. A bias voltage is applied between the sample and the tip.

Atomic Forces. When the tip is very close to the surface, as in Figure 1a, there is an overlap in the wave functions of the tip and the surface, giving rise to atomic forces. Such atomic forces were first used to slide Xe atoms on Ni(110) at 4 K to form an "IBM" logo where each letter was written by a collection of atoms.[20] Similarly, a linear array of Xe atoms was assembled.[20] These initial experiments were followed by the manipulation of CO on Pt(111) to form different patterns consisting of collections of CO molecules,[21] as well as the manipulation of Pt atoms on Pt(111)[21] and the creation of a circular arrangement of Fe atoms on Cu(111).[22,23] More recently, much larger molecules were pushed by the STM tip. Most notably, the manipulations were carried out at room temperature and include the repositioning of a porphyrin molecule with four bulky hydrocarbon groups ("legs") on Cu(100)[24] and the sliding of C_{60} molecules to control their positions on Cu(111).[25] By increasing the strength of the tip−surface interaction, more tightly bound atoms of a metal surface, Cu(211), were detached and reattached elsewhere on the surface at room temperature.[26,27] The manipulation of single atoms, molecules, and dimers on Cu(211) has also been demonstrated.[28]

Tunneling Electrons. The atomic forces diminish as the tip−surface separation increases and become insignificant when this separation reaches about 6 Å. This is the typical separation for chemical modifications by tunneling electrons as shown in Figure 1b. Tunneling electrons were used to reversibly transfer a Xe atom between a polycrystalline tungsten tip and a Ni(110) surface.[29] The tunneling current takes on two values depending on whether the Xe atom is on the tip or the surface, hence the name "atomic switch". The rate of transfer was found to depend nonlinearly on the tunneling current, with an exponent of 4.9 ± 0.2. By applying a larger bias voltage (>2.4 V), it was possible to transfer a more tightly bonded CO on Cu(111) to the tip with a rate that depended linearly on current.[30] Desorption of H atoms from Si(100)-2 × 1 surface was used to generate patterns (parallel and crossed lines) by scanning the tip at bias voltages greater than 2 V.[6,31,32] A significant isotope effect was observed; the desorption yield of D was found to be about 2 orders of magnitude lower than that of H.[32] By using tunneling instead of field-emitted electrons, line widths down to the dimensions of a Si−Si dimer were demonstrated.

Electric Field. Chemical bonds can be perturbed by sufficiently strong electric fields. The strength of the electric field between the tip and the surface is significant due to the close proximity of the tip to the surface, and it can be comparable to the field that the electrons experience in atoms and molecules ($\sim 10^8$ V cm^{-1}). The field pattern is difficult to quantify and depends on the shape and atomic arrangement of the tip (which are not accurately known), the tip−surface separation, and the applied bias. As Figure 1c implies, the extent of the field is larger than atomic dimensions. However, the threshold field required for surface modification can naturally lead to confinement of the modifications. The strength of the electric field is expected to be highest for the part of the tip closest to the surface; thus it is possible to achieve

atomically resolved modifications on the surface. The electric field has been used to dissociate Si−Si bonds on Si(111)-7 × 7,[33−35] to deposit hydrogen atoms on Si(111)-7 × 7,[36] to move Cs atoms laterally on the (110) surfaces of GaAs and InSb,[37] and to rotate antimony dimers[38] and Si ad-dimers[39] on Si(100) surface.

Field-Emitted Electrons. When the bias voltage exceeds the work function of the tip (4.5 eV for W), field emission of electrons occurs. To avoid an exceedingly large current, the tip−surface separation is increased to 10−20 Å so that a significantly larger area is irradiated (∼ 50−100 Å diameter), as shown in Figure 1d.[40] Therefore, modifications with field-emitted electrons are not confined to atomic dimensions.

The dissociation of an isolated decaborane(14) ($B_{10}H_{14}$) adsorbed on Si(111)-7 × 7 at room temperature into fragments was induced by electrons from the STM tip by scanning an area including the adsorbed molecule with the sample biased at ≥4 V.[41] Using the same scanning method, with the bias at ≥6 V, dissociation of O_2 on Si-(111)-7 × 7 at room temperature was observed.[42]

Methodology of Bond-Selected Chemistry with Tunneling Electrons

Control and induction of bond selected chemistry is best achieved with tunneling electrons. First, the initial excitation by tunneling electrons is confined to atomic dimensions (<1 Å), allowing bond selectivity. Second, the magnitude and energy of the tunneling electrons can be varied to control the reaction rate and pathways. Since the bias voltages are typically below 1 V (or equivalently the energies of the tunneling electrons are below 1 eV), localized and controlled reaction can be carried out. For example, the dissociation of a single O_2 molecule on Pt-(111) is confined to the molecule if the bias is less than 0.5 V.[9] However, when the bias is increased to 1.0 V, molecules as far as 100 Å away are dissociated even though the electrons are confined to atomic dimensions.[9] The detailed mechanism for this nonlocal effect is not yet understood. Similar observations have been made on the desorption of NO and the dissociation of H_2S and D_2S on Si(111)-7 × 7 at 50 K.[43] Bias voltages larger than about 2.5 V lead to nonlocal chemistry, whereas single-molecule chemistry takes place for bias voltages of 1−2 V.[43] This nonlocal chemistry on Si could also be due to a mechanism involving the extended range of the electric field.

The junction conductance depends very sensitively on the atomic configuration in the tunnel junction. In Figure 2a, the dissociation of a chemical bond is schematically shown to lead to two states of the current, corresponding to before and after bond dissociation. The moment of dissociation is detected as a rapid change in the current. The dissociation of single O_2 on Pt(111) exhibits the process shown in Figure 2a.[9] Similarly, in Figure 2b, the tunneling current is used to induce and monitor the motion of a single atom on the surface. The tunneling current can also cause the same atom to move back to the original position. Thus the time-dependent tunneling current exhibits the property of a bistable switch, as demonstrated by single-atom manipulation on Si(111)-7 × 7 at 50 K.[44]

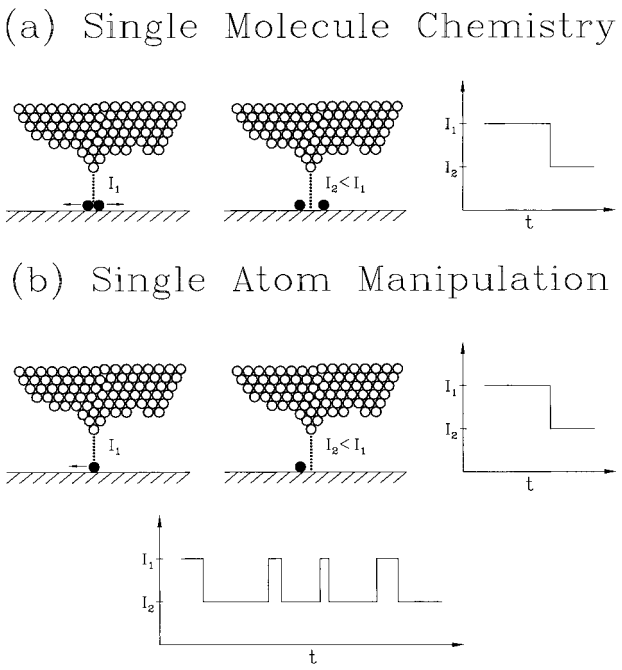

FIGURE 2. Schematic showing the sudden change in the tunneling current at the moment of (a) single molecule dissociation, and (b) single atom manipulation. The recurrent bistable switching of the tunneling current between I_1 and I_2 corresponds to the two states with the atom directly within and away from the tunneling electrons.

There are a number of experimental requirements for carrying out bond-selected chemistry with tunneling electrons. The molecules need to be fixed in position on the surface in order for the STM to track the molecule and position the tip to inject electrons in a precisely chosen point of the molecule. Since molecules tend to be mobile and diffuse on the surface, the STM needs to operate with the sample regulated below room temperature. Our STM (microscope, electronics, and software) is homemade and operates in ultrahigh vacuum (2×10^{-11} Torr). The temperature of the STM and the sample can be varied over the range 8−350 K. Tracking of a chosen point of the surface (molecule) can be controlled to within 0.1 Å in the $x-y$ plane and within 0.01 Å in the z direction. Data acquisition is under computer control. In the following, the concept of bond-selected chemistry with tunneling electrons is illustrated with two reactions studied in our laboratory.

Unimolecular Reaction: Single-Molecule Dissociation and Desorption

Oxygen on Pt(111).[9] The system of oxygen on Pt(111) exhibits properties that make it a good model for revealing and understanding the fundamental mechanisms and dynamics of surface chemistry. For example, oxygen on Pt(111) has played a key role in our fundamental understanding of surface photochemistry.[45] When adsorbed alone, photodesorption and photodissociation occur,

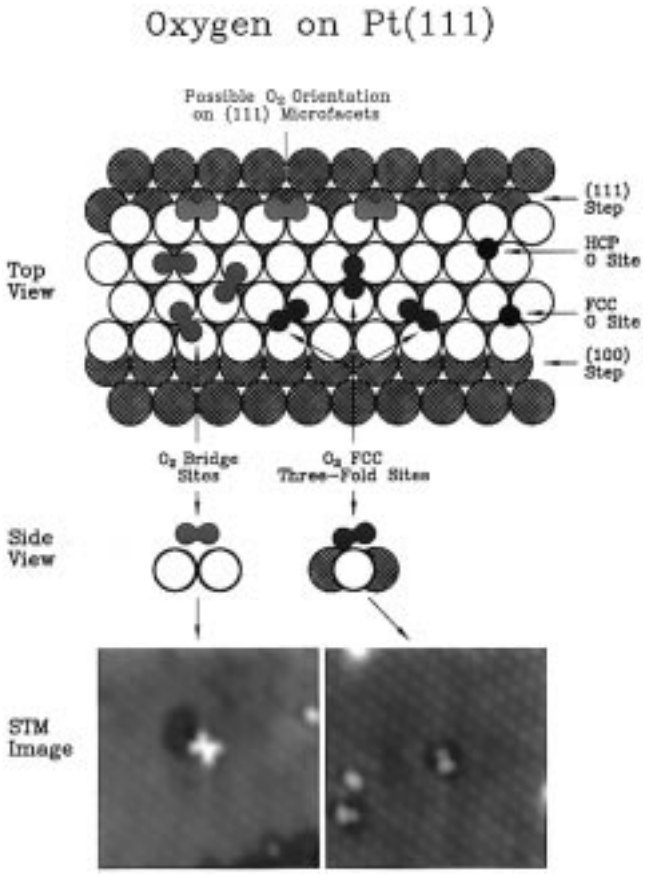

FIGURE 3. Schematic showing the molecular and atomic oxygen adsorbed on Pt(111) as observed by variable-temperature STM. The oxygen molecules on the 2-fold bridge and 3-fold fcc sites have three equivalent orientations; STM images are shown for one orientation.

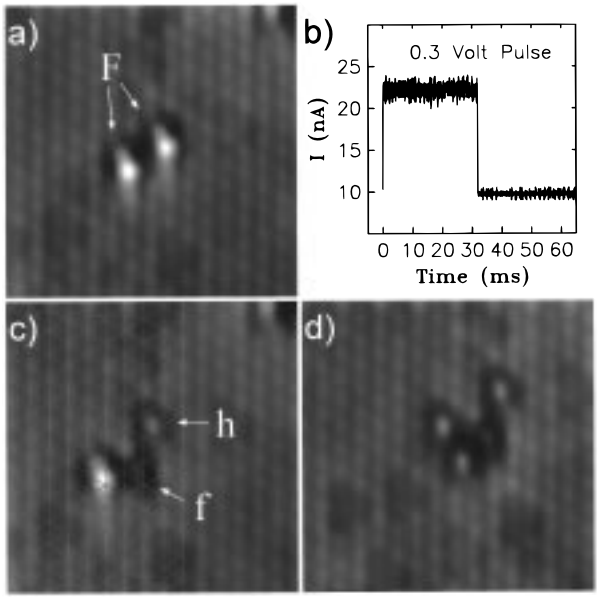

FIGURE 4. Example of single-bond dissociation. (a) STM image of two adjacent O_2 molecules adsorbed on fcc 3-fold hollow sites of Pt(111) at 50 K. (b) Tunneling current vs time during a 0.3 V pulse over the O_2 molecule on the right; sudden change at 30 ms is the moment of dissociation. (c) STM image after dissociation showing one O atom on fcc site, f, and the other on hcp site, h. (d) STM image taken after applying a second pulse over the remaining molecule, showing dissociation into two O atoms on hcp sites. The tip is about 6 Å above each molecule during the pulse. Reprinted with permission from ref 9. Copyright 1997 The American Physical Society.

which are prototypes for unimolecular reactions. Coadsorption of O_2 and CO on Pt(111) leads to photon-induced bimolecular reaction yielding CO_2, in direct competition with the photodesorption and photodissociation of O_2. Similarly, oxygen on Pt(111) also provides us with a rich model system to explore bond-selected chemistry with tunneling electrons.[9]

It is known that oxygen adsorbs molecularly on Pt(111) at temperatures below 100 K.[46] When the temperature is increased to about 150 K, desorption of O_2 is detected with a mass spectrometer. The remaining molecules dissociate and the oxygen atoms recombine and desorb as O_2 starting at about 600 K. The bonding configurations of molecular and atomic oxygen on Pt(111) as determined by low-temperature STM (8−350 K) are shown in Figure 3.[9,47] These different atomic and molecular oxygen species have been imaged individually and in islands. The thermodynamically stable atomic O resides in face-centered cubic (fcc) 3-fold hollow sites; O atoms on the hexagonal close-packed (hcp) sites are metastable and can only be created nonthermally by irradiation with electrons or photons.[47] No molecules are observed at (100) steps.

We have studied the dissociation induced by tunneling electrons of single O_2 molecules on the bridge and 3-fold hollow sites of Pt(111).[9] Figure 4a is an image of two oxygen molecules adsorbed on fcc 3-fold hollow sites on Pt(111) at 50 K. The adjacent atoms of the underlying Pt atoms on the (111) surface are spaced by 2.77 Å; the observed separation of the two molecules is 5.54 Å. The STM tip was then positioned about 6 Å above one of the molecules (the top right one) and a voltage pulse of 0.3 V and 100 ms duration was applied. Figure 4b shows a tunneling current of 22 nA before and 9.5 nA after the dissociation of O_2. The sudden change in the tunneling current indicates the moment of dissociation. A repeat of such measurement over many single molecules yields an exponential distribution of the time duration between the initiation of excitation ($t = 0$) and this moment. The dissociation rate is the inverse of the time constant of this distribution. The image taken after the dissociation, Figure 4c, shows the two O products, one on the hcp site and the other on the fcc site, as well as the other O_2 molecule, which is not perturbed. Figure 4d shows the four O atoms, one on the fcc site and three on the hcp sites, after the second molecule has been dissociated in a similar manner. Atoms on the hcp sites can be moved to fcc sites by applying a voltage pulse; the site transfer in the reverse direction has not been observed. The energy of the hcp-site O atoms is theoretically estimated to be 0.4 eV higher than fcc-site O atoms.[48]

The two O products are found to be within two lattice constants of the original molecule and one to three lattice constants apart. Approximately 1.1 eV/O atom of energy is dissipated upon dissociation through substrate excitations. The rates of energy dissipation and scattering with

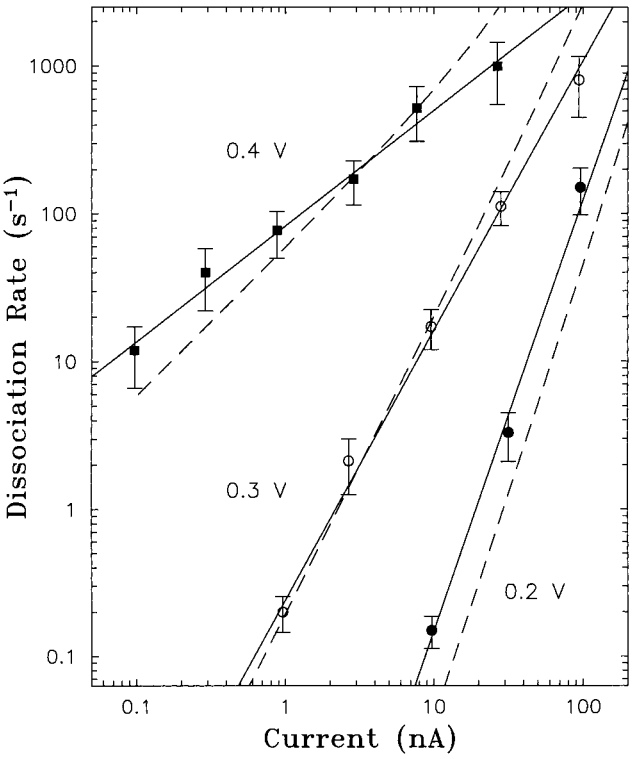

FIGURE 5. Dissociation rate as a function of tunneling current for three bias voltages of single O_2 molecules adsorbed on fcc 3-fold hollow sites on Pt(111) at 50 K. The solid lines are fits to the data and the dashed lines are results from theoretical modeling. Reprinted with permission from ref 9. Copyright 1997 The American Physical Society.

the corrugated potential of the surface limit the range of motion of the products.[49]

A single O_2 molecule in the fcc 3-fold hollow site can be transformed into bridge bonded molecule by displacing it with the STM tip. The reverse transformation is also observed.[9,47] While dissociation only is observed for O_2 on the fcc sites, dissociation competes with desorption for O_2 bonded on bridge sites. Molecular O_2 bonded at steps are also found to desorb. Higher bias voltages are required for perturbing the single O_2 molecule on bridge and step sites compared to those on 3-fold sites, due to the higher binding energies.

The mechanisms and the dynamics of single-bond dissociation are revealed by measuring the dissociation rate as a function of bias voltage and tunneling current and by theoretical modeling of the data.[9] Results obtained for the dissociation of single O_2 molecules on fcc 3-fold sites are shown in Figure 5. The dissociation rate has a power law dependence on the tunneling current, $\propto I^N$, with experimental values of $N = 0.8 \pm 0.2$, 1.8 ± 0.2, and 2.9 ± 0.3 as compared to theoretical values of 1.17, 2.07, and 3.13, respectively.[9]

The proposed mechanism is based on inelastic vibrational excitations of an adsorbed molecule by the tunneling electrons.[50−52] Such a process is illustrated schematically in Figure 6. A tunneling electron inelastically scatters from an adsorbed molecule and transfers energy to the vibrational modes of the molecule. In order for the O−O

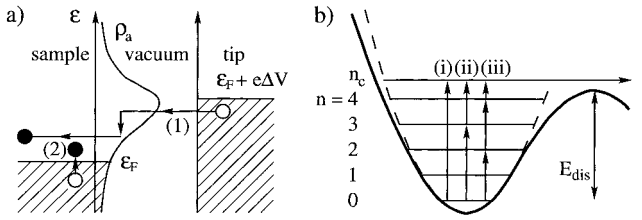

FIGURE 6. Schematic depicting the essential steps in the theoretical modeling of single O_2 molecule dissociation on Pt(111). (a) Inelastic electron scattering via an O_2 resonance, ρ_a (1). Vibrational relaxation occurs due to electronic excitations within the substrate (2). (b) Transitions that lead to dissociation for (i) 0.4, (ii) 0.3, and (iii) 0.2 V bias voltages. A truncated harmonic oscillator is used; E_{dis} is the dissociation barrier. Reprinted with permission from ref 9. Copyright 1997 The American Physical Society.

bond to break, an energy barrier of 0.35−0.38 eV needs to be overcome via one or multiple vibrational excitations in the ground electronic state. Such a vibrational ladder-climbing process requires one or multiple inelastic scatterings. For 0.4 V bias, the O_2 molecule can be dissociated with a single inelastic scattering event, thus the linear dependence on the current. However, at least two scatterings are required for 0.3 V bias, which accounts for $N = 2$. The discrete (quantized) nature of the vibrational levels requires three scatterings for 0.2 V bias, thus $N = 3$.

Implicitly, the vibrational ladder climbing process depicted in Figure 6b occurs via the minimum number of vibrational transitions.[52] This results from consideration of the relative rates of inelastic excitation and vibrational relaxation. The excitation rate is determined by the magnitude of the tunneling current, which varies from 0.1 to 100 nA in Figure 5. Taking a diameter of 1 Å for the tunneling current, the scattering rates are 6×10^8 to 6×10^{11} electrons Å^{-2} s^{-1}. The relaxation rate of the O−O stretch vibration on Pt(111) is calculated from the infrared vibrational line shape to be $\sim 4 \times 10^{12}$ s^{-1}.[53] Thus the vibrational relaxation rate is greater than the excitation rate. The most likely path to dissociation is therefore the one with the minimum relaxation probability, which is clearly the path with the fewest transitions. For 0.4 V bias, the bound-to-continuum transition corresponds to a single excitation to overcome the dissociation barrier of 0.35−0.38 eV. In contrast, in the atomic switch involving Xe atom transfer between the W tip and the Ni(110) surface,[29] the excitation rate exceeds the vibrational relaxation rate. The tunneling current is in the range 20−200 nA, which corresponds to scattering rates $\sim 10^{11}-10^{12}$ electrons Å^{-2} s^{-1}, while the vibrational relaxation rate of Xe on Ni is $\sim 3 \times 10^{10}$ s^{-1}. In the high current and/or low vibrational relaxation regime the dissociation rate is dominated by multiple single-step vibrational excitations within the ground electronic state.[50−52] The desorption of H or D from Si surface also lies in this regime.[6,31,32]

Single-Atom Manipulation

Displacement of Si Adatoms.[44] The top layer of the Si(111)-7 × 7 surface contains 12 adatoms in the unit cell, as shown in Figure 7e, which are imaged in Figure 7a by

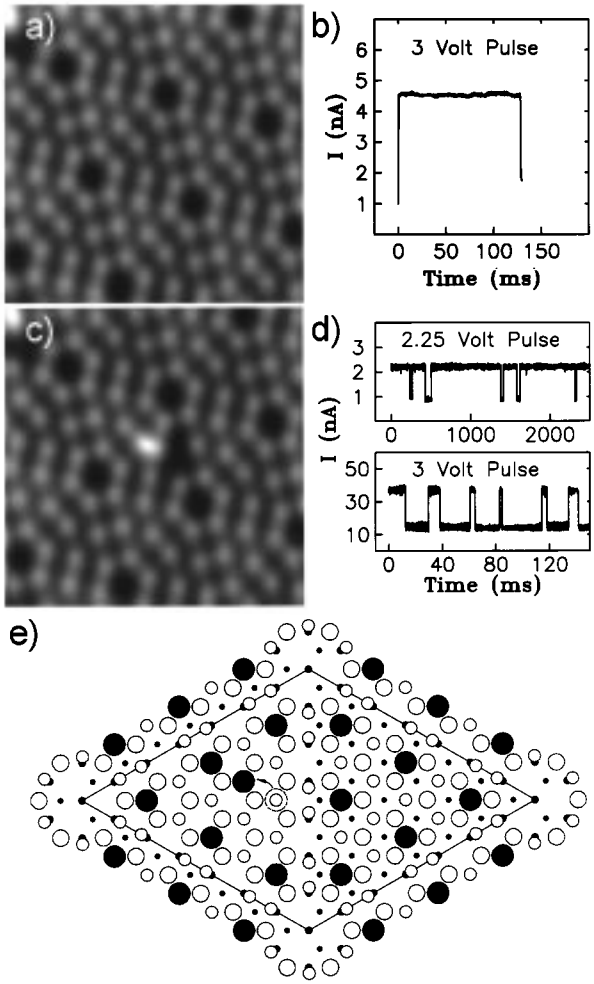

FIGURE 7. Single-atom manipulation on Si(111)-7 × 7 at 50 K. (a) STM image of the clean surface. (b) A 3 V pulse is applied over a center adatom and is discontinued when a sudden change in the tunneling current is sensed. (c) STM image taken after application of voltage pulse shown in panel b. (d) Bistable switching in tunneling current, corresponding to single atom motion directly within (high) and away (low) from the region of tunneling electrons. (e) Schematic of the 7 × 7 unit cell showing the hopping of a center adatom in panel c. This single atom hopping is reversible and continues as long as the voltage pulse is applied.

the STM. There are 6 adatoms in each half of the unit cell, and within each half, there are 3 center adatoms and 3 corner adatoms. The corner adatoms form small six-membered rings and the center adatoms form the next larger diameter rings. Positioning the tunneling current directly over a center adatom in the faulted half of the unit cell (i.e., the left half in Figure 7e) induces displacement of the adatom. Figure 7b shows the application of a 3 V bias pulse and 4.5 nA of current over a center adatom; the moment of its displacement is indicated by a sudden drop in the current. An STM image taken after the displacement is displayed in Figure 7c and a schematic showing the displacement is presented in Figure 7e. As can be seen in Figure 7b, the voltage pulse is ended as soon as the displacement occurs in order to prevent current-induced return of the adatom. Such reversible displacement−return events are shown in Figure 7d where the voltage pulse is allowed to continue. The current assumes bistable values. The high and low values correspond to the adatom directly within and away from the tunneling electrons, respectively. This switching action was illustrated schematically in Figure 2b. The durations in the high and low current states are dependent on the bias voltage; the return rate is greater than the displacement rate at 2.25 V, while the opposite is true for 3 V and higher biases. It is also found that the atomic displacement rate depends linearly on the current, which indicates a mechanism involving single electronic excitation of silicon back-bonds.

Future Prospects

The ability to image reactants and products in addition to inducing bond-selected chemistry provides us with unprecedented control and understanding of chemistry. The possibility of manipulating atoms and molecules on surfaces makes it possible to study environmental effects on chemical reactions. While only unimolecular surface reactions have been demonstrated, the induction of bimolecular reactions and the study of more complex ensemble effects should be possible. Questions arise as to the feasibility of initiating a reaction in a chosen bond of a polyatomic molecule and the degree to which this initial excitation is distributed energetically to other parts of the molecule and to the substrate. The demonstration of single-bond vibrational spectroscopy would significantly advance the chemical sensitivity of atomically resolved scanning probes. The combination of the wavelength tunability of the laser and the spatial resolution of the STM could lead to new possibilities in the field of single-molecule spectroscopy, dynamics, and chemistry. There is currently a general interest in exploring chemical, biological, and materials systems at the atomic and molecular scales. Recent advances in STM made it possible to induce and view the motions of single adsorbed molecules, thus providing an unprecedented opportunity to explore chemistry at the spatial limit.

It is a great pleasure and learning experience for me to work with Barry C. Stipe and Mohammad A. Rezaei on the STM. I am also greatly indebted to Shiwu Gao and Mats Persson for the theoretical understanding during their visits to Cornell. This research would not have been possible without support by the National Science Foundation under Grant DMR-9417866 and the Department of Energy under Grant DE-FG02-91ER14205.

References

(1) Herschbach, D. R. *Angew. Chem., Int. Ed. Engl.* **1987**, *26*, 1221−1243. Lee, Y. T. *Science* **1987**, *236*, 793−798.
(2) Zewail, A. H. *Femtochemistry: Ultrafast Dynamics of the Chemical Bond, Volumes I and II*; World Scientific: Singapore, 1994.
(3) Feynman, R. P. *Engineering and Science* **1960**, February, 22−36; California Institute of Technology: Pasadena, CA, 1960.
(4) Binning, G.; Rohrer, H.; Gerber, Ch.; Weibel, E. *Phys. Rev. Lett.* **1982**, *49*, 57−61.
(5) Stroscio, J. A.; Eigler, D. M. *Science* **1991**, *254*, 1319−1326.

(6) Avouris, Ph. *Acc. Chem. Res.* **1995**, *28*, 95−102.
(7) Binning, G.; Quate, C. F.; Gerber, Ch. *Phys. Rev. Lett.* **1986**, *56*, 930−933.
(8) Hamers, R. J. *J. Phys. Chem.* **1996**, *100*, 13103−13120.
(9) Stipe, B. C.; Rezaei, M. A.; Ho, W.; Gao, S.; Persson, M.; Lundqvist, B. I. *Phys. Rev. Lett.* **1997**, *78*, 4410−4413.
(10) Crewe, A. V.; Langmore, J. P.; Isaacson, M. S. In *Physical Aspects of Electron Microscopy and Microbeam Analysis*; Siegel, B. M., Beaman, D. R., Eds.; Wiley: New York, 1975; pp 47−62.
(11) Pennycook, S. J.; Boatner, L. A. *Nature* **1988**, *336*, 565−567.
(12) Muller, E. W. *Z. Phys.* **1951**, *131*, 136−142.
(13) Isaacson, M. S. *Ultramicroscopy* **1989**, *28*, 320−323.
(14) Muller, D. A.; Silcox, J. *Philos. Mag. A* **1995**, *71*, 1375−1387.
(15) Stroscio, J. A., Kaiser, W. J., Eds. *Scanning Tunneling Microscopy*; Academic Press: San Diego, CA, 1993.
(16) Binnig, G.; Rohrer, H.; Gerber, Ch.; Weibel, E. *Appl. Phys. Lett.* **1982**, *40*, 178−180.
(17) Sautet, P.; Joachim, C.; Bocquet, M. L.; Salmeron, M. *Ann. Chim. Sci. Mater.* **1992**, *17*, 217−227; Sautet, P. *Surf. Sci.* **1997**, *374*, 406−417.
(18) Lang, N. D. *Surf. Sci.* **1994**, *299/300*, 284−297.
(19) Tersoff, J.; Lang N. D. In *Scanning Tunneling Microscopy*; Stroscio, J. A., Kaiser, W. J., Eds.; Academic Press: San Diego, CA, 1993; pp 1−29.
(20) Eigler, D. M.; Schweizer, E. K. *Nature* **1990**, *344*, 524−526.
(21) Zeppenfeld, P.; Lutz, C. P.; Eigler, D. M. *Ultramicroscopy* **1992**, *42*−*44*, 128−133.
(22) Crommie, M. F.; Lutz, C. P.; Eigler, D. M. *Science* **1993**, *262*, 218−220.
(23) Heller, E. J.; Crommie, M. F.; Lutz, C. P.; Eigler, D. M. *Nature* **1994**, *369*, 464−466.
(24) Jung, T. A.; Schlittler, R. R.; Gimzewski, J. K.; Tang, H.; Joachim, C. *Science* **1996**, *271*, 181−184.
(25) Cuberes, M. T.; Schlittler, R. R.; Gimzewski, J. K. *Appl. Phys. Lett.* **1996**, *69*, 3016−3018.
(26) Meyer, G.; Zophel, S.; Rieder, K.-H. *Phys. Rev. Lett.* **1996**, *77*, 2113−2116.
(27) Meyer, G.; Bartels, L.; Zophel, S.; Henze, E.; Rieder, K.-H. *Phys. Rev. Lett.* **1997**, *78*, 1512−1515.
(28) Bartels, L.; Meyer, G.; Rieder, K.-H. *Phys. Rev. Lett.* **1997**, *79*, 697−700.
(29) Eigler, D. M.; Lutz, C. P.; Rudge, W. E. *Nature* **1991**, *352*, 600−603.
(30) Bartels, L.; Meyer, G.; Rieder, K.-H.; Velic, D.; Knoesel, E.; Hotzel, A.; Wolf, M.; Ertl, G. *Phys. Rev. Lett.* **1998**, *80*, 2004−2007.
(31) Shen, T.-C.; Wang, C.; Abeln, G. C.; Tucker, J. R.; Lyding, J. W.; Avouris, Ph.; Walkup, R. E. *Science* **1995**, *268*, 1590−1592.
(32) Avouris, Ph.; Walkup, R. E.; Rossi, A. R.; Shen, T.-C.; Abeln, G. C.; Tucker, J. R.; Lyding, J. W. *Chem. Phys. Lett.* **1996**, *257*, 148−154.
(33) Lyo, I.-W.; Avouris, Ph. *Science* **1991**, *253*, 173−176.
(34) Avouris, Ph.; Lyo, I.-W. *Appl. Surf. Sci.* **1992**, *60/61*, 426−436.
(35) Salling, C. T.; Lagally, M. G. *Science* **1994**, *265*, 502−506.
(36) Kuramochi, H.; Uchida, H.; Aono, M. *Phys. Rev. Lett.* **1994**, *72*, 932−935.
(37) Whitman, L. J.; Stroscio, J. A.; Dragoset, R. A.; Cellota, R. *Science* **1991**, *251*, 1206−1210.
(38) Mo, Y. W. *Science* **1993**, *261*, 886−888.
(39) Swartzentruber, B. S.; Smith, A. P.; Jonsson, H. *Phys. Rev. Lett.* **1996**, *77*, 2518−2521.
(40) Mayer, T. M.; Adams, D. P.; Marder, B. M. *J. Vac. Sci. Technol. B* **1996**, *14*, 2438−2444.
(41) Dujardin, G.; Walkup, R. E.; Avouris, Ph. *Science* **1992**, *255*, 1232−1235.
(42) Martel, R.; Avouris, Ph.; Lyo, I.-W. *Science* **1996**, *272*, 385−388.
(43) Rezaei, M. A.; Stipe, B. A.; Ho, W., to be published [NO, H_2S, D_2S on Si(111)-7 × 7].
(44) Stipe, B. A.; Rezaei, M. A.; Ho, W. *Phys. Rev. Lett.* **1997**, *79*, 4397−4400.
(45) Ho, W. In *Laser Spectroscopy and Photochemistry on Metal Surfaces, Parts I and II*; Dai, H.-L., Ho, W., Eds.; World Scientific: Singapore, 1995; pp 1047−1140.
(46) Gland, J. L.; Sexton, B. A.; Fisher, G. B. *Surf. Sci.* **1980**, *95*, 587−602.
(47) Stipe, B. A.; Rezaei, M. A.; Ho, W. *J. Chem. Phys.* **1997**, *107*, 6443−6447.
(48) Feibelman, P. J.; Esch, S.; Michely, T. *Phys. Rev. Lett.* **1996**, *77*, 2257−2260.
(49) Wahnstrom, G.; Lee, A. B.; Stromquist, J. *J. Chem. Phys.* **1996**, *105*, 326−336.
(50) Gao, S.; Persson, M.; Lundqvist, B. I. *Solid State Commun.* **1992**, *84*, 271−273; *Phys. Rev. B* **1997**, *55*, 4825−4836.
(51) Walkup, R. E.; Newns, D. M.; Avouris, Ph. *Phys. Rev. B* **1993**, *48*, 1858−1861.
(52) Salam, G. P.; Persson, M.; Palmer, R. E. *Phys. Rev. B* **1994**, *49*, 10655−10662.
(53) Persson, B. N. J. *Chem. Phys. Lett.* **1987**, *139*, 457−462.

AR9501784